Iranian Journal of Fuzzy Systems

Volume 16, Number 4, (2019), pp. 97-114

University of Sistan and Baluchestan

Doppler and bearing tracking using fuzzy adaptive unscented Kalman filter

S. H. Hashemi[1] and A. R. Alfi[2]

[1] *Faculty of Electrical and Robotic Engineering, Shahrood University of Technology, Iran*

a_ alfi@shahroodut.ac.ir

Abstract

The topic of Doppler and Bearing Tracking (DBT) problem is to achieve a target trajectory using the Doppler and Bearing measurements. The difficulty of DBT problem comes from the nonlinearity terms exposed in the measurement equations. Several techniques were studied to deal with this topic, such as the unscented Kalman filter. Nevertheless, the performance of the filter depends directly on the prior knowledge, involving the accurate model, sufficient information of the noise distribution and the suitable initialization. To address these problems, in this paper, a new adaptive factor together with a fuzzy logic system is proposed for online adjusting the process and the measurement noise covariance matrices simultaneously. In the core of the proposed algorithm, the fault detection procedure is also adopted to reduce the computational time. The theoretical developments are investigated by simulations, which indicate the effectiveness of the proposed filter in DBT problem.

Keywords: Doppler and bearing tracking, unscented Kalman filter, fuzzy logic system, fault detection.

1 Introduction

Passive target tracking concerns with the estimation problem of the target position and velocity using a signal emitted solely from it [33]. Target tracking based on bearing measurements has gained considerable attention in recent years [17]. In the Bearing Only Tracking (BOT) problem, it is generally assumed that the target is moving with a constant velocity. In addition, the maneuvering of the observer must be such that the observability condition is satisfied to realize a feasible solution. Once the source emits the harmonic components, the harmonic signals will experience Doppler shifts at the observer such that the frequency measurements can be used to achieve better estimation accuracy. The combined use of Doppler shifts and bearing angles for analyzing a moving target is so-called Doppler and Bearing Tracking (DBT). In DBT problem, there is no need to maneuver the observer for achieving a determinant solution. This is the main advantage of DBT in comparison with BOT.

The main topic in DBT problem is the nonlinearity of the measurement equations. To address this issue, different techniques were reported in the literature, such as the pseudo-linear technique, the maximum likelihood (ML), and the instrumental variable (IV). In [23], the two-step pseudo-linear technique was studied for DBT using a time reference point in the middle of the data record. However, there was a large bias in the parameters estimation. In [27], the ML estimation, which is a highly nonlinear technique with respect to the unknown parameters, was adopted to achieve an unbiased solution. The Gradient search techniques, such as the quasi-Newton, was normally used for optimizing the ML function. In [18], the performance of IV technique was investigated for reducing the bias. However, this method can not be used in online estimation since it is a batch algorithm. Furthermore, increasing the number of measurements leads to increasing the computational time. The recursive IV technique was employed to reduce the strong bias generated by the pseudo-linear formation [3]. Although, the recursive least square method was developed for decreasing the bias effects, there was still dependence on initial conditions like other recursive algorithms [7]. In addition, the particle filters were tested in DBT to achieve higher tracking accuracy in camparison with the conventional filters [28]. Although, high

Corresponding Author: A. R. Alfi
Received: May 2018; Revised: July 2018; Accepted: December 2018.

computational burden is the main shortcoming of such filters [35]. Another common technique for solving the DBT problem is the Kalman filter and its variants, for example, the modified gain extended Kalman filter [22], the unscented Kalman filter (UKF) [24], the range parameterized unscented Kalman filter [13], the iterated unscented Kalman filter [34], and the extended Kalman filter (EKF) [19].

A critical limitation of the Kalman filter is that a priori knowledge of the stochastic errors for the process and measurement models must be available [12]. This is a complex task in practical problems, since the noise statistics is usually time-varying. Furthermore, in a variable task environment, such as ocean, the target dynamic is uncertain. Also, the modified versions of Kalman filter, namely the EKF and the UKF, suffer from some disadvantages including the linearization, nonlocal sampling (in a high state-space dimension), and negative semi-definite covariance matrix problems. The EKF has poor performance in DBT problem due to linearization leading to highly unstable filter, wherein assumptions of the local linearity are violated [36]. The UKF as a traditional filtering algorithm has satisfactory performance for the estimation of high nonlinearity problems. However, the conventional UKF algorithm has no capability to adapt itself to the faults in the process noise or the measurement noise [26]. In the EKF and UKF, constant values of the process and measurement noise covariance matrices frequently require during the estimation process. This is a trial-and-error method for the first time, which is a very time-consuming and error-prone task.

To cope with these problems, several adaptive techniques were discussed for adjusting the covariance matrices [14, 30, 2, 4]. In [25, 15], the measurement and process noise covariance matrices with adaptive factors were tuned. Fuzzy logic were used for online tuning of the measurement noise covariance matrix [10, 16, 32]. In [37], the MIT rule was studied to derive an adaptive law for tuning the measurement noise covariance matrix. In [11, 21], the UKF and the Adaptive UKF (AUKF) were adopted for reducing the initial condition sensitivity. In comparison with EKF, the AUKF has less reliance on the prior covariance statistical information as well as an automatic calculation of the process and measurement noise covariance matrices [8]. Hence, the observer cannot be restricted by initial noise covariance matrices, and therefor, the AUKF gives a suitable performance for the estimation of time-varying and nonlinear systems. It is usual in the adaptive techniques that only one of the process or measurement noise covariance matrices is adjusted. Accordingly, there is still an open area to enhance the performance of UKF.

Having these ideas in mind, the purpose of this paper is to introduce a fuzzy adaptive UKF (FAUKF) algorithm to deal with the DBT problem. The main contributions of this paper lie in the following aspects: 1) a new adaptive factor is proposed for online tuning process noise covariance matrix, 2) a fuzzy logic system is embedded for adjusting the measurement noise covariance matrix, due to high nonlinearity variation in this matrix. In the core of the proposed FAUKF, the fault detection procedure [6] is also adopted for decreasing the computational time.

The rest of this paper is organized as follows. The state and measurement equations are described in Section 2. The UKF is explained in section 3. The proposed algorithm is introduced in Section 4. Simulation results are given in Section 5. Finally, conclusions are outlined in Section 6.

2 State and measurement equations

Figure 1 shows the general scheme of the DBT problem [3]. In this Figure, the subscript T and O stand for the target and observer, respectively, $x(t), \dot{x}(t)$ and $y(t), \dot{y}(t)$ denote the position and velocity, respectively, $b(t)$ is the bearing angle, and f_B is the constant unknown target frequency.

From Figure 1, the true bearing angle from the observer to the target $b(t)$ is obtained as

$$b(t) = \tan^{-1}\left(\frac{x_T(t) - x_O(t)}{y_T(t) - y_O(t)}\right). \tag{1}$$

In case the target and the observer have relative motions, the frequency measured by the observer $f_r(t)$ is given by [3]

$$f_r(t) = f_B\left(1 + \frac{V_D}{C}\right) \tag{2}$$

where C is the propagation speed of the tone signal and V_D is the target radial velocity with respect to the observer, which can be expressed in terms of the target and the observer velocities as [7]

$$V_D = (\dot{x}_O(t) - \dot{x}_T(t)) \times \sin(b(t)) + (\dot{y}_O(t) - \dot{y}_T(t)) \times \cos(b(t)). \tag{3}$$

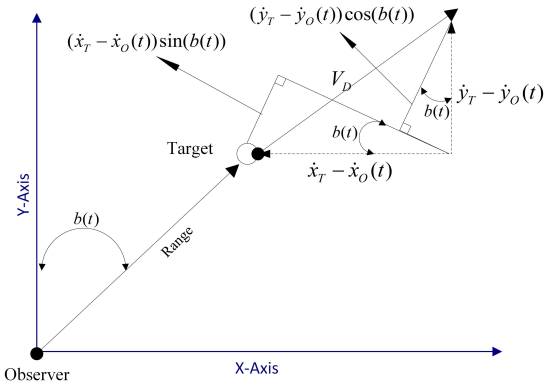


Figure 1: Doppler-bearing tracking [3].

The set of measured data consists of two types of measurements, including the bearing angle and the frequency.

$$Y(t) = \begin{bmatrix} b(t) \\ f_r(t) \end{bmatrix} \tag{4}$$

The target is supposed to be moving with a constant velocity and the following state vector.

$$X(t) = \begin{bmatrix} x(t) \\ \dot{x}(t) \\ y(t) \\ \dot{y}(t) \\ f_B \end{bmatrix} \tag{5}$$

Since the target moves in a straight line with a constant velocity, the transient matrix should be linear in the form of equation (6), where Δ is the time step.

$$F = \begin{bmatrix} 1 & \Delta & 0 & 0 & 0 \\ 0 & 1 & 0 & 0 & 0 \\ 0 & 0 & 1 & \Delta & 0 \\ 0 & 0 & 0 & 1 & 0 \\ 0 & 0 & 0 & 0 & 1 \end{bmatrix} \tag{6}$$

3 Unscented Kalman filter

The Kalman filter, which is the most well-known filter, is an optimal estimator for linear systems under the Gaussian distribution and white noise. To extend the Kalman filter for nonlinear systems, different types of this algorithm, namely the EKF and the UKF, were introduced in the literature. The UKF has many advantages over the EKF [1], particularly in the problems with high nonlinearity properties [9]. The state distribution was also approximated by a Gaussian random variable (GRV) represented using a minimal set of sample points. These sample points were opted to capture the estimated mean and covariance of the GRV. When the sample points were propagated through the nonlinear system under study, the posterior mean and covariance can be approximated by the second order of Taylor series expansion.

Let us define the state vector x with mean $\hat{x}(k|k)$ and covariance $P(k|k)$, which undergoes the nonlinear function $y = h(x)$. Consider the following discrete-time nonlinear system.

$$x_{k+1} = f(x_k, k) + w_k \tilde{y}_k = h(x_k, k) + v_k \tag{7}$$

where x_k and $\tilde{y}_k$ are the state and the measurement vectors, respectively. Moreover, w_k and v_k are the process and measurement noises, respectively, which are the Gaussian white noise with covariance $Q(k)$ and $R(k)$.

The first step in UKF is to create $2n+1$ sigma points, where n denotes the dimension of the state vector in the following relationship.

$$\begin{aligned} x_0(k|k) &= \hat{x}(k|k) \\ x_i(k|k) &= \hat{x}(k|k) + (\sqrt{(n+\beta)P(k|k)})_i, i = 1 \dots n \\ x_i(k|k) &= \hat{x}(k|k) - (\sqrt{(n+\beta)P(k|k)})_i, i = n+1 \dots 2n \end{aligned} \tag{8}$$

In equation (8), $x_0(k|k)$ and $x_i(k|k)$ are the sigma points, $(\sqrt{(n+\beta)P(k|k)})_i$ is the i^{th} row of the matrix square root, and β is the scaling factor satisfying $n+\beta = 3$ [9].
The next step is propagating these sigma points through the nonlinear dynamic equation, which is called the transient matrix in the linear case.

$$\tilde{x}_i(k+1|k) = f\left[x_i(k|k), k\right], i = 0 \cdots 2n \tag{9}$$

These propagated points are then used to obtain the predicted mean and covariance as expressed in equation (10).

$$\begin{aligned} \hat{x}(k+1|k) &= \frac{1}{n+\beta}\left\{\beta\tilde{x}_0(k+1|k) + \frac{1}{2}\sum_{i=1}^{2n}\tilde{x}_i(k+1|k)\right\} \\ P(k+1|k) &= \frac{1}{n+\beta}\Big\{\beta[\tilde{x}_0(k+1|k) - \hat{x}(k+1|k)][\tilde{x}_0(k+1|k) - \hat{x}(k+1|k)]^T \\ &+\frac{1}{2}\sum_{i=1}^{2n}[\tilde{x}_i(k+1|k) - \hat{x}(k+1|k)][\tilde{x}_i(k+1|k) - \hat{x}(k+1|k)]^T\Big\} + Q(k) \end{aligned} \tag{10}$$

where $\hat{x}(k+1|k)$ and $P(k+1|k)$ are the predicted mean and covariance, respectively.
The next step is recreation of the sigma points with the predicted mean given by [2]

$$\begin{aligned} x_0(k+1|k) &= \hat{x}(k+1|k) \\ x_i(k+1|k) &= \hat{x}(k+1|k) + (\sqrt{(n+\beta)P(k+1|k)})_i, i = 1 \dots n \\ x_i(k+1|k) &= \hat{x}(k+1|k) - (\sqrt{(n+\beta)P(k+1|k)})_i, i = n+1 \dots 2n \end{aligned} \tag{11}$$

Afterward, these points undergo the nonlinear measurement equations and the gain predicted measurements as

$$\begin{aligned} y_i(k+1|k) &= h\left[x_i(k+1|k), k\right], i = 0 \cdots 2n \\ \hat{y}(k+1|k) &= \frac{1}{n+\beta}\left\{\beta y_0(k+1|k) + \frac{1}{2}\sum_{i=1}^{2n} y_i(k+1|k)\right\}. \end{aligned} \tag{12}$$

The measurement covariance matrix is

$$\begin{aligned} P_{yy}(k+1|k) = \frac{1}{n+\beta}\Big\{&\beta[y_0(k+1|k) - \hat{y}(k+1|k)][y_0(k+1|k) - \hat{y}(k+1|k)]^T \\ &+\frac{1}{2}\sum_{i=1}^{2n}[y_i(k+1|k) - \hat{y}(k+1|k)][y_i(k+1|k) - \hat{y}(k+1|k)]^T\Big\} \end{aligned} \tag{13}$$

and the innovation covariance matrix is given by

$$P_{vv}(k+1|k) = P_{yy}(k+1|k) + R(k).$$

(14)

The cross correlation matrix is also determined by equation (15).

$$P_{xy}(k+1|k) = \frac{1}{n+\beta}\Big\{\beta[x_0(k+1|k) - \hat{x}(k+1|k)][y_0(k+1|k) - \hat{y}(k+1|k)]^T + \frac{1}{2}\sum_{i=1}^{2n}[x_i(k+1|k) - \hat{x}(k+1|k)][y_i(k+1|k) - \hat{y}(k+1|k)]^T\Big\} \tag{15}$$

The Kalman gain is then computed as

$$K(k+1) = P_{xy}(k+1|k)P_{vv}^{-1}(k+1|k). \tag{16}$$

Finally, the estimated state and covariance matrices are obtained as follow.

$$\begin{aligned}\hat{x}(k+1|k+1) &= \hat{x}(k+1|k) + K(k+1)(y(k+1) - \hat{y}(k+1|k))\\ P(k+1|k+1) &= P(k+1|k) - K(k+1)P_{vv}(k+1|k)K^T(k+1)\end{aligned} \tag{17}$$

4 The proposed adaptive methods

Improper process and measurement noise covariance matrices often result in a large estimation error or even the divergence of the filter [31]. Indeed, determining appropriate values of these matrices is a time-consuming and complex work [29]. Consequently, the performance of the observer based on EKF may not be satisfactory in practice. The main purpose of this paper is to improve the performance of the observer in DBT problem. To address this problem, the FAUKF algorithm is proposed for online tuning of the process and measurement noise covariance matrices simultaneously.

4.1 Tuning $R(k)$ using fuzzy logic

The performance of UKF under complete information of the measurement noise is outstanding. This assumption is unrealistic in practical cases since the environment is time-varying and statistics of the noise cannot be exactly obtained. In this research work, a fuzzy system is incorporated into the UKF in order to amend measurement noise adaptively. The performance of UKF is investigated by the residual. Using the incoming $\tilde{y}_k$ and the predicted measurements $\hat{y}_k$, the residual is defined as [5]

$$r_k = \tilde{y}_k - \hat{y}_k. \tag{18}$$

The residual has two covariance matrices, namely the theoretical and the actual, indicating the degree of divergence. The theoretical covariance matrix in UKF is equal to the innovation covariance matrix P_{vv} and the actual covariance matrix of residual is defined as

$$C_r = \frac{1}{m}\sum_{i=k-m+1}^{k} r_i \times r_i^T \tag{19}$$

where m is the size of estimating window.
A ratio of trace between the actual and theoretical covariance matrices specifies the performance of the filter, denoted by Degree of Matching (DOM) [16].

$$DOM = \frac{Tr(C_r)}{Tr(P_{vv})} \tag{20}$$

where $Tr(.)$ is the matrix trace.
Therefore, it is possible to evaluate the performance of the filter using DOM. The filter works in the optimal circumstance when these two covariance matrices are equal, that is, $DOM = 1$. Accordingly, the variation of DOM can be considered as the input of fuzzy system. Furthermore, the measurement noise covariance matrix R has a direct relationship with innovation covariance matrix P_{vv}. Thus, adjusting the matrix R leads to regulation of matrix P_{vv}. Accordingly, the output of fuzzy system $q(k)$ can be considered to regulate the matrix R as

$$R(k+1) = q(k) \times R(k). \tag{21}$$

The linguistic meanings of the input and output membership functions are (L=Less, E=Equal, F=Further), (D= Decrease, M=Maintain, I=Increase), respectively. From definition of the input and output fuzzy sets, the following IF-THEN rules are defined.

Rule 1: If DOM is L then $q(k)$ is D.

Rule 2: If DOM is E then $q(k)$ is M.

Rule 3: If DOM is F then $q(k)$ is I.

The Gaussian membership functions are also chosen for having smooth variations. Using the Mamdani fuzzy system with singleton fuzzification, product method for the inference and centroid method for the defuzzification, the crisp output can be determined as

$$y = \frac{\sum_{l=1}^{m} \prod_{i=1}^{n} \mu_{A_i^l}(x_i) \bar{y}_l}{\sum_{l=1}^{m} \prod_{i=1}^{n} \mu_{A_i^l}(x_i)} \tag{22}$$

where m is the number of rules, n is the number of fuzzy inputs, $\mu_{A_i^l}(x_i)$ is the membership functions, and $\bar{y}_l$ is the centroid of the membership functions [20].

4.2 The proposed new adaptive factor

In UKF, the sigma points capture the mean and covariance of the prior estimation. The factor β is used for scaling the sigma points for improving the performance of the estimation. In other words, the sigma points can be scaled toward or away from the prior estimation. Let define $|x_i - \hat{x}|$ as the distance between the i^{th} sigma point (x_i) and the predicted mean ($\hat{x}$), which is related to $\sqrt{n+\beta}$ as shown in equation (8). Three values can be considered for this factor, namely $\beta > 0$ for scaling away, $\beta < 0$ for scaling toward, and $\beta = 0$ for no scaling. In general, it is recommended to opt $n + \beta = 3$ [9]. However, in case $\beta = 3 - n < 0$, it can result in the negative semi-definite covariance matrix [9].

To solve this problem, here, a new adaptive factor for tuning the process noise covariance matrix Q is proposed. This is because of this matrix has a straightforward relevance with the predicted covariance matrix P. From equation (8), it is apparent that the matrix P has a direct relationship with sigma points scaling as well. Using equation (17), let consider the difference between the predicted mean and estimated states as

$$\delta(k) = \hat{x}(k+1|k+1) - \hat{x}(k+1|k) = K(k+1)(y(k+1) - \hat{y}(k+1|k)). \tag{23}$$

Since prediction of the filter has a direct relation with the sigma point scaling, one rational way for improvement of the filter performance is tuning the sigma points scaling. As mentioned before, the sigma point scaling can be regulated by tuning of the process noise covariance matrix Q, leading to the improvement of the filter prediction. Hence, the following adaptive factor for adjusting the matrix Q is defined.

$$\lambda = \frac{1}{n} \sum_{i=1}^{n} \frac{1}{\delta_i^2(k) + \alpha} Q(k+1) = \lambda \times Q(k) \tag{24}$$

where α is a small positive constant and n is the dimension of the state vector.

4.3 Fault detection

Fault detection procedure was studied formerly for diagnosing the threshold of the estimation error [6]. Here, this method is adopted into the proposed FAUKF. In order to avoid increasing the computational time, this procedure is recommended to distinguish when the usage of the fuzzy system is necessary for reducing the estimation error. In the fault detection, a statistical function is computed at each step, which is expressed by [6]

$$\gamma(k) = r^T(k+1)[P_{yy}(k+1|k) + R(k+1)]^{-1} r(k+1). \tag{25}$$

This function has χ^2 distribution with τ degree of freedom, where τ is the dimension of the residual vector. If the level of significance σ is selected as

$$P(\chi^2 > \chi^2_{\sigma,\tau} = \sigma; 0 < \sigma < 1) \tag{26}$$

then, the threshold value $\chi^2_{\sigma,\tau}$ is determined. Therefore, two hypotheses can be considered as follows.

H1) $\gamma(k) \leq \chi^2_{\sigma,\tau}$; the estimation error is satisfactory, and use of the fuzzy system is not required.

H2) $\gamma(k) > \chi^2_{\sigma,\tau}$; the estimation error is not satisfactory, and use of the fuzzy system is required.

Figure 2 shows the flow chart of the proposed algorithm.

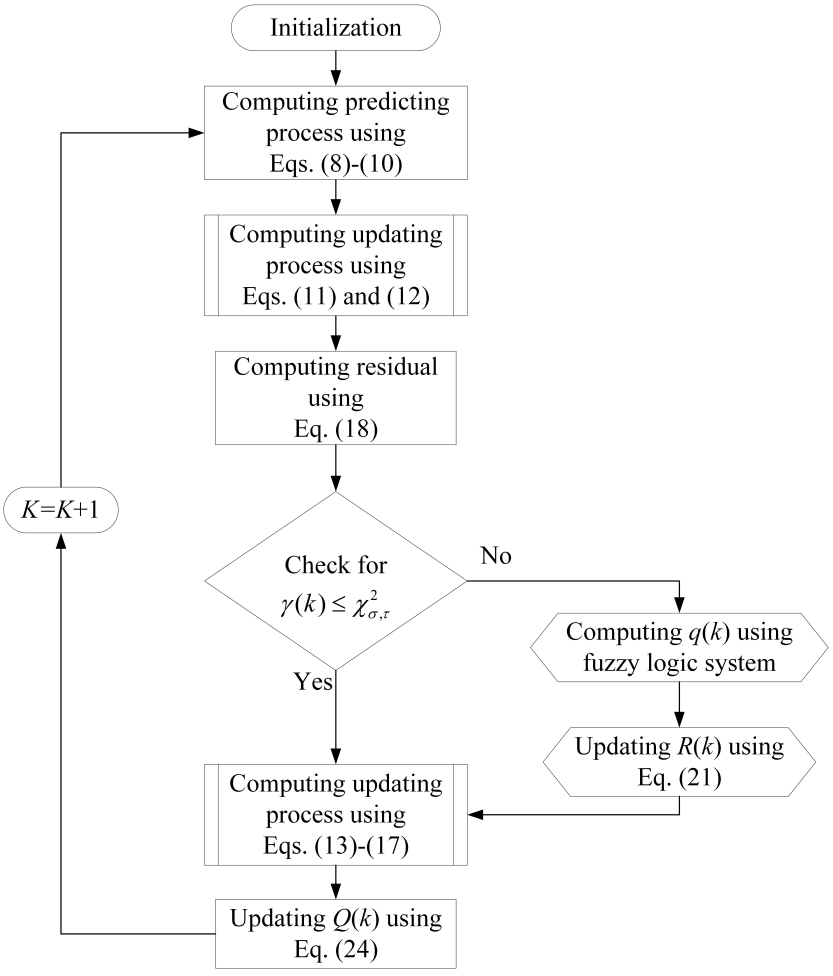


Figure 2: Flow chart of the proposed FAUKF.

5 Simulation

To assess the performance of the proposed FAUKF in comparison with standard UKF (SUKF), three experiments are carried out. In the first experiment, just process noise covariance matrix Q is tuned by the new adaptive factor. The purpose of this experiment is to show the effect of this factor on the performance of the filter. In the second one, both matrices Q and R are adjusted simultaneously. In this experiment, two different tests are performed with/without the fault detection procedure. The goal is to evaluate the effect of this procedure on the computational time. To further assess, the third experiment is provided with different conditions. The same scenario is used for the first and second experiments as listed in Table 1. In these experiments, it is assumed that the target and observer velocities are constant, the target radiation frequency is 500 Hz, and the frequency and bearing measurements are corrupted by zero mean white Gaussian noises with $\sigma_f^2 = (0.3Hz)^2$ and $\sigma_\beta^2 = (2 \times \frac{\pi}{180} rad)^2$, respectively. The sampling time is set to 1 sec and the filter is executed 2000 sec based on the Monte Carlo simulation. The number of Monte Carlo runs is 100. It is worth pointing out that the initial conditions are selected for the optimal performance of SUKF. All simulations are conducted by the MATLAB 2015a language on a 2.5 GHz, 5CPU Pentium-based computer operating under Windows 7. Initial values of the process and measurement noise covariance matrices are chosen as

$$Q = 10^{-4} \times I_{5\times 5}, R = \begin{bmatrix} 0.017 & 0 \\ 0 & 0.6 \end{bmatrix}.$$

Table 1: Simulation table for the first and second experiments.

Target initial position (m)	6×10^3,6×10^3
Observer initial position (m)	0,0
Target course (deg)	170
Observer course (deg)	100
Target velocity (knot)	15
Observer velocity (knot)	5

5.1 First experiment

In this experiment, the performance of SUKF is compared with AUKF, whereas only the matrix Q is adjusted using the new adaptive factor. Simulation results are given in Figures 3, 4, 5, 6. Figures 3 and 4 display the observer, target and estimation of the filter's with corresponding errors, respectively. These Figures demonstrate that the new adaptive factor can decrease the convergence time and estimation errors. Figure 5 shows the estimated bearing and frequency errors. Velocity and course estimation errors are illustrated in Figure 6. From these results, it can be concluded that the new adaptive factor for tuning the process noise covariance can improve the performance of UKF properly.

In order to assess the performance of the filter in terms of accuracy, the following Root Mean Square Error (RMSE) is considered as an appropriate objective function

$$RMSE = \frac{1}{n_t} \sum_{t=1}^{n_t} \sqrt{\frac{1}{k} \sum_{i=1}^{k} (x(t) - \hat{x}(t))^2} \tag{27}$$

where $x(t)$ and $\hat{x}(t)$ denote the true state of the target and its estimation, respectively, k is the number of Monte Carlo runs and n_t is the simulation time.
The results are summarized in Table 2.

Table 2: Mean errors in the first experiment.

Filter type	SUKF	AUKF
Position error (m)	2303.6	1904.9
Bearing error (deg)	0.005	0.005
Frequency error (Hz)	0.031	0.025
Course error (deg)	49.83	47.21
Speed error (m/s)	3.55	3.16

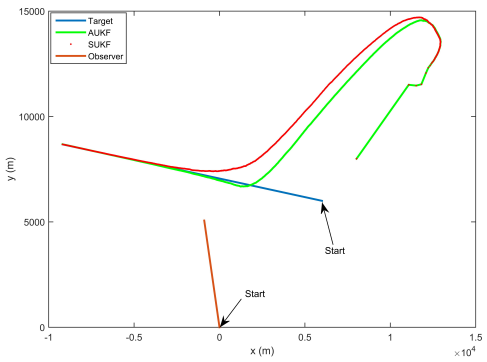


Figure 3: Position trajectory in the first experiment.

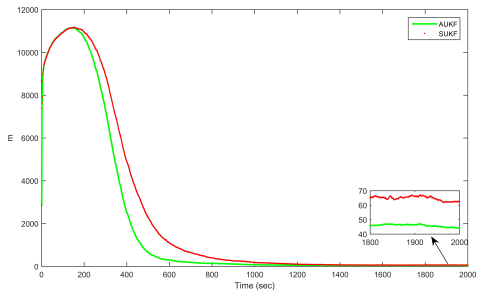


Figure 4: Position error in the first experiment.

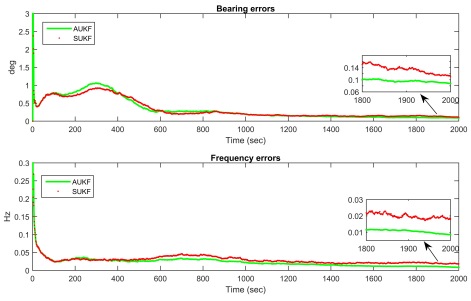


Figure 5: Bearing and frequency errors in the first experiment.

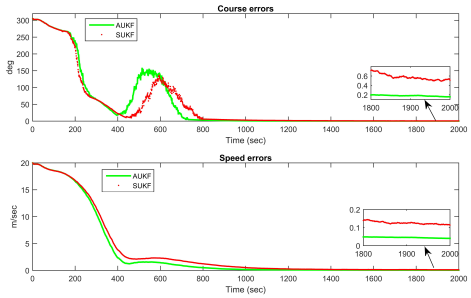


Figure 6: Course and speed errors in the first experiment.

5.2 Second experiment

Here, the performance of the proposed FAUKF with/without fault detection procedure is compared with the SUKF and the AUKF. The goal of this experiment is to study the effect of the fault detection procedure on the computational time. Figures 7 and 8 depict the fuzzy input and output membership functions, respectively. As expected, simulation results show the proper performance of the FAUKF in the problem under study. Table 3 lists mean parameters estimation errors during the simulation. From this experiment, it can be deduced that use of the fuzzy system into the AUKF improves the filter performance in terms of accuracy.

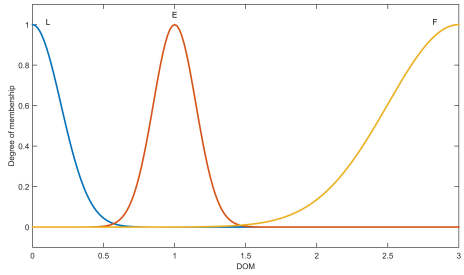


Figure 7: Fuzzy logic input membership function.

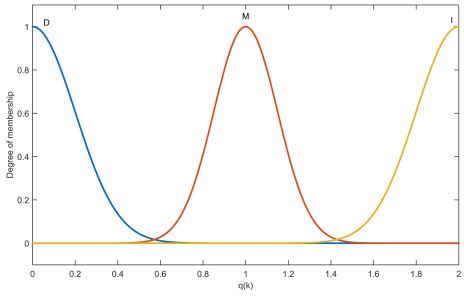


Figure 8: Fuzzy logic output membership function.

Figures 9 and 10 illustrate the target, observer, and filter's estimation together with corresponding errors, respectively. The bearing, frequency, velocity and course estimation errors are illustrated in Figures 11 and 12, respectively. From these Figures, the least estimation error is obtained by the proposed FAUKF. Note that the aim of this experiment is to evaluate the performance of the proposed FAUKF in terms of the computational time. Figure 15 depicts the target, observer and filter's estimated trajectories and Figure 16 shows their corresponding errors. These results indicate that the performance of the proposed filter without fault detection procedure is outstanding. Figures 17 and 18 exhibit bearing, frequency, velocity and course estimation errors. Referring to Figures 13, 14, it can be seen that increasing the fetch of fuzzy function leads to increasing the computational time.

Table 3: Mean errors with fault detection procedure in the second experiment.

Filter type	SUKF	AUKF	FAUKF
Position error (m)	1577	1550.1	1284.5
Bearing error (deg)	0.006	0.006	0.004
Frequency error (Hz)	0.022	0.02	0.02
Course error (deg)	29.1	29.04	27.98
Speed error (m/s)	2.28	2.21	2

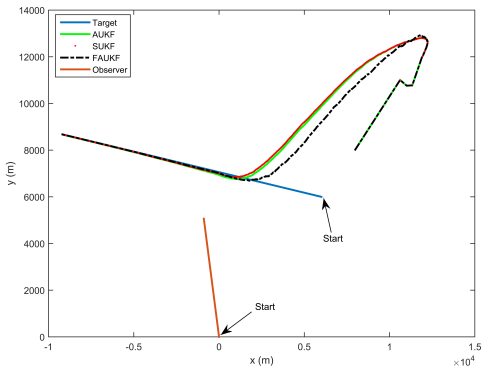


Figure 9: Position trajectory in the second experiment without fault detection.

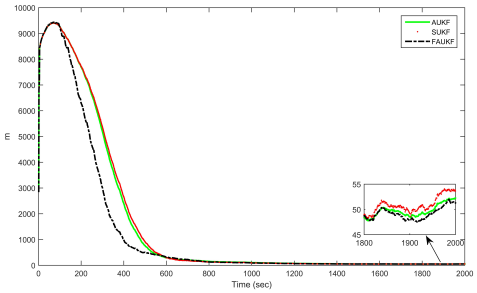


Figure 10: Position error in the second experiment without fault detection.

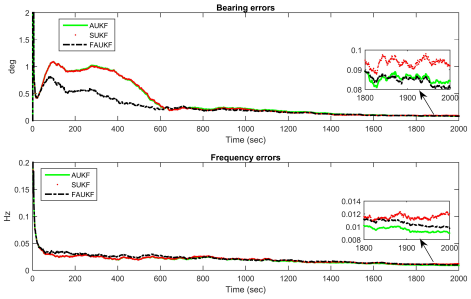


Figure 11: Bearing and frequency errors in the second experiment without fault detection.

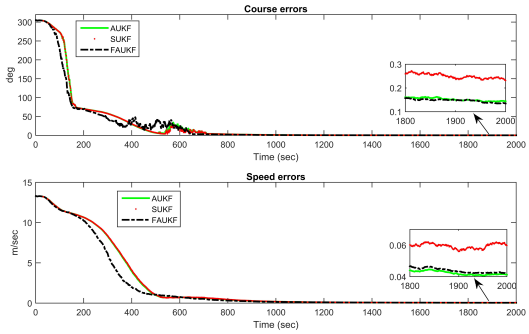


Figure 12: Course and speed errors in the second experiment without fault detection.

Profile Summary

Generated 28-Feb-2018 19:13:12 using cpu time.

Function Name	Calls	Total Time	Self Time*	Total Time Plot (dark band = self time)
Flogic	1255	1.711 s	0.108 s	
h	60000	1.608 s	0.577 s	
ukf_FA	2000	1.456 s	0.345 s	
ukf_A	2000	1.355 s	0.389 s	
ukf	2000	1.263 s	0.280 s	
evalfis	1255	0.779 s	0.077 s	
wrapToPi	64000	0.747 s	0.438 s	
ukf_mean_covariance	12000	0.634 s	0.634 s	
isfis	1255	0.609 s	0.016 s	
cell.ismember	1255	0.593 s	0.062 s	
wrapTo360	72000	0.391 s	0.391 s	
addmf	12550	0.375 s	0.375 s	
cell.unique	2510	0.330 s	0.109 s	
updatex	60000	0.329 s	0.329 s	
wrapTo2Pi	64000	0.310 s	0.310 s	
ukf_covariance	6000	0.300 s	0.300 s	
addrule	1255	0.232 s	0.032 s	
cell.unique>celluniqueR2012a	2510	0.221 s	0.221 s	
ismember	1255	0.202 s	0.030 s	
ukf_sigmapoints	6000	0.189 s	0.189 s	
ismember>ismemberR2012a	1255	0.172 s	0.063 s	
addvar	2510	0.155 s	0.155 s	
getfis	2510	0.109 s	0.109 s	

Figure 13: Computational time in the second experiment with fault detection.

Profile Summary

Generated 28-Feb-2018 19:17:32 using cpu time.

Function Name	Calls	Total Time	Self Time*	Total Time Plot (dark band = self time)
Flogic	1976	3.058 s	0.092 s	
h	60000	1.423 s	0.655 s	
evalfis	1976	1.417 s	0.110 s	
ukf_FA	2000	1.375 s	0.500 s	
ukf	2000	1.312 s	0.215 s	
ukf_A	2000	1.309 s	0.230 s	
isfis	1976	0.932 s	0.046 s	
cell.ismember	1976	0.886 s	0.184 s	
addmf	19760	0.877 s	0.877 s	
ukf_mean_covariance	12000	0.657 s	0.657 s	
wrapToPi	64000	0.531 s	0.374 s	
cell.unique	3952	0.499 s	0.234 s	
ukf_covariance	6000	0.380 s	0.380 s	
addrule	1976	0.375 s	0.063 s	
wrapTo360	72000	0.301 s	0.301 s	
updatex	60000	0.296 s	0.296 s	
ukf_sigmapoints	6000	0.295 s	0.295 s	
cell.unique>celluniqueR2012a	3952	0.265 s	0.265 s	
addvar	3952	0.234 s	0.234 s	
ismember	1976	0.203 s	0.016 s	
setfis	1976	0.202 s	0.202 s	
ismember>ismemberR2012a	1976	0.187 s	0.079 s	
evalfismex (MEX-file)	1976	0.173 s	0.173 s	

Figure 14: Computational time in the second experiment without fault detection.

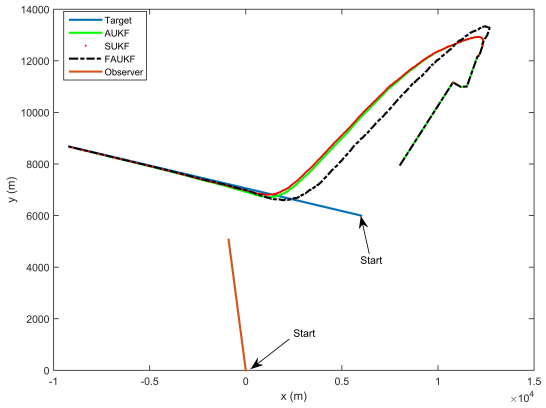


Figure 15: Position trajectory in the second experiment with fault detection.

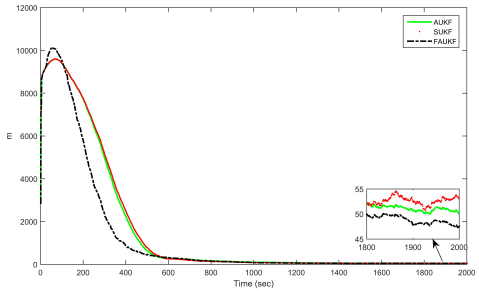


Figure 16: Position error in the second experiment with fault detection.

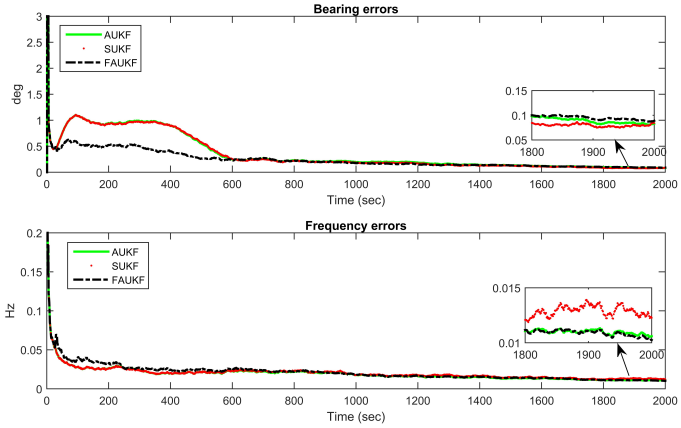


Figure 17: Bearing and frequency errors in the second experiment with fault detection.

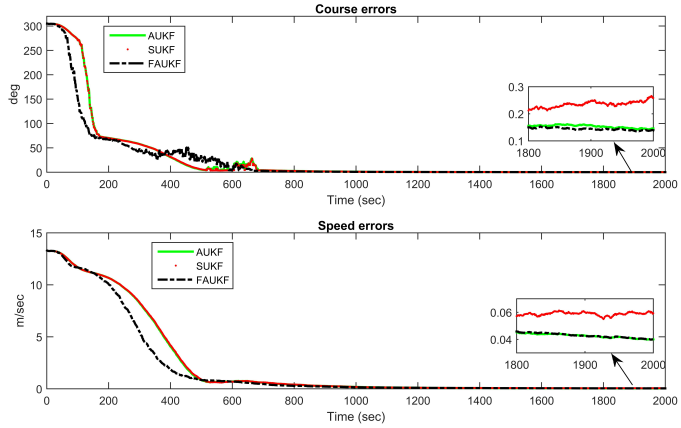


Figure 18: Course and speed errors in the second experiment with fault detection.

Table 4 summarizes the mean parameters estimation errors during the simulation time, which indicate the proper performance of the proposed FAUKF.

Table 4: Mean errors in the second experiment without fault detection procedure.

Filter type	SUKF	AUKF	FAUKF
Position error (m)	1586.9	1559.1	1264.3
Bearing error (deg)	0.006	0.006	0.004
Frequency error (Hz)	0.02	0.02	0.02
Course error (deg)	29.24	29.41	26.27
Speed error (m/s)	2.27	2.25	1.96

5.3 Third experiment

In this experiment, different scenarios are considered in DBT problem. Simulation table for this experiment is shown in Table 5. Here, the target and observer move with a constant velocity and course. The target radiation frequency is set to 1000 Hz. The frequency and bearing measurements are corrupted by zero mean white Gaussian noises with $\sigma_f^2 = (0.6Hz)^2$ and $\sigma_\beta^2 = (4 \times \frac{\pi}{180} rad)^2$, respectively. Figures 19, 20, 21, 22 depict the results corresponding to the third experiment. Results reveal the appropriate performance of the proposed FAUKF in DBT problem.

$$Q = 10^{-4} \times I_{5\times 5}, R = \begin{bmatrix} 0.034 & 0 \\ 0 & 1 \end{bmatrix}$$

Table 5: Simulation table for the third experiment.

Target initial position (m)	6×10^3,6×10^3
Observer initial position (m)	0,0
Target course (deg)	290
Observer course (deg)	10
Target velocity (knot)	12
Observer velocity (knot)	6

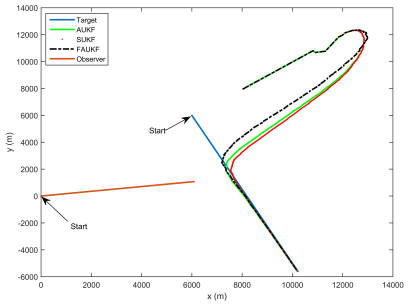


Figure 19: Position trajectory in the third experiment.

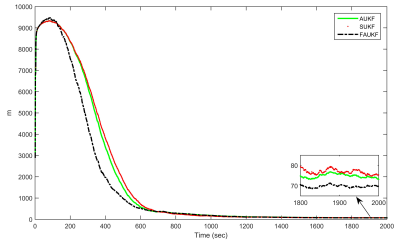


Figure 20: Position error in the third experiment.

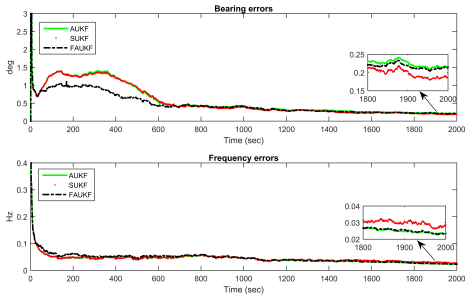


Figure 21: Bearing and frequency errors in the third experiment.

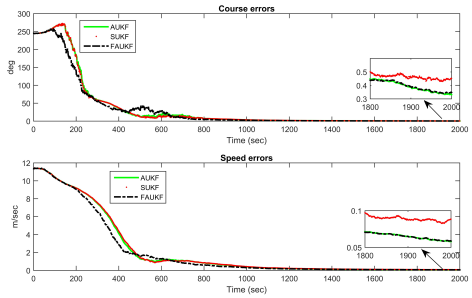


Figure 22: Course and speed errors in the third experiment.

In summary, from the results of the first experiment, it can be concluded that the new adaptive factor has the direct effect on the UKF performance. The second experiment confirms that embedding the fuzzy logic system can improve the performance of the filter, leading to increasing the computational time. Then, the fault detection procedure is adopted to reduce the computational time. In the third experiment, the feasibility of the algorithm was evaluated in different conditions. Results indicate satisfactory performance of the proposed algorithm in the problem under study.

Table 6: Mean errors in the third experiment.

Filter type	SUKF	AUKF	FAUKF
Position error (m)	1823.3	1783.6	1555.7
Bearing error (deg)	0.01	0.01	0.008
Frequency error (Hz)	0.04	0.03	0.03
Course error (deg)	35.75	36.26	33.69
Speed error (m/s)	2.22	2.18	2

6 Conclusions

This paper proposed two different adaptation methods for UKF algorithm to deal with the DBT problem. In order to reduce the dependence on initial conditions on the performance of UKF, the measurement and process noise covariance matrices were adjusted simultaneously during the filter operation. To this end, two systematic manners were proposed. First, the fuzzy logic system for regulating the measurement noise covariance matrix was introduced. Second, the new adaptive factor for tuning the process noise covariance matrix was defined. The fault detection procedure was also used for reducing the computational time caused by the fuzzy system. Finally, the validity and feasibility of the proposed filter was verified via different numerical simulation examples.

References

[1] A. Alkaya, *Unscented Kalman filter performance for closed-loop nonlinear state estimation: a simulation case study*, Electrical Engineering, **96**(4) (2014), 299-308.

[2] E. Cao, K. Jiang, *Adaptive unscented Kalman filter for input estimations in Diesel-engine selective catalytic reduction systems*, Neurocomputing, **205** (2016), 329-335.

[3] Y. Chan, S. Rudnicki, *Bearings-only and Doppler-bearing tracking using instrumental variables*, IEEE Transactions on Aerospace and Electronic Systems, **28**(4) (1992), 1076-1083.

[4] G. Dikic, Z. Djurovic, *Unbiased estimation of atmosphere attenuation coefficient*, Electrical Engineering, **89**(4) (2007), 343-347.

[5] P. Escamilla-Ambrosio, N. Mort, *Adaptive Kalman filtering through fuzzy logic*, Proceedings of the 7th UK Workshop On Fuzzy Systems, Recent Advances and Practical Applications of Fuzzy, Neuro-Fuzzy, and Genetic Algorithm-Based Fuzzy Systems, (2000), 26-27.

[6] C. Hajiyev, H. E. Soken, *Robust adaptive unscented Kalman filter for attitude estimation of pico satellites*, International Journal of Adaptive Control and Signal Processing, **28**(2) (2014), 107-120.

[7] K. Ho, Y. Chan, *An asymptotically unbiased estimator for bearings-only and Doppler-bearing target motion analysis*, IEEE Transactions on Signal Processing, **54**(3) (2006), 809-822.

[8] K. Jiang, E. Cao, L. Wei, *NOx sensor ammonia cross-sensitivity estimation with adaptive unscented Kalman filter for Diesel-engine selective catalytic reduction systems*, Fuel, **165** (2016), 185-192.

[9] S. J. Julier, J. K. Uhlmann, *New extension of the Kalman filter to nonlinear systems*, Signal processing, sensor fusion, and target recognition VI. International Society for Optics and Photonics, **3068** (1997), 182-194.

[10] D. Jwo, S. Lai, *Navigation integration using the fuzzy strong tracking unscented Kalman filter*, The Journal of Navigation, **62**(2) (2009), 303-322.

[11] D. J. Jwo, C. H. Tseng, *Fuzzy adaptive interacting multiple model unscented Kalman filter for integrated navigation*, Control Applications,(CCA) and Intelligent Control,(ISIC), (2009), 1684-1689.

[12] D. J. Jwo, C. F. Yang, C. H. Chuang, T. Y. Lee, *Performance enhancement for ultra-tight GPS/INS integration using a fuzzy adaptive strong tracking unscented Kalman filter*, Nonlinear Dynamics, **73**(1-2) (2013), 377-395.

[13] S. Koteswara Rao, *Doppler-bearing passive target tracking using a parameterized unscented kalman filter*, IETE Journal of Research, **56**(1) (2010), 69-75.

[14] D. Lee, G. Vukovich, R. Lee, *Robust adaptive unscented Kalman filter for spacecraft attitude estimation using quaternion measurements*, Journal of Aerospace Engineering, **30**(4) (2017), 9-17.

[15] K. Z. Liu, J. Li, W. Guo, P. Q. Zhu, X. H. Wang, *Navigation system of a class of underwater vehicle based on adaptive unscented Kalman fiter algorithm*, Journal of Central South University, **22**(2) (2014), 550-557.

[16] X. Liu, H. J. Liu, Y. G. Tang, Q. Gao, Z. M. Chen, *Fuzzy adaptive unscented Kalman filter control of epileptiform spikes in a class of neural mass models*, Nonlinear Dynamics, **76**(2) (2014), 1291-1299.

[17] N. Nguyen, K. Dogancay, *Improved pseudolinear Kalman filter algorithms for bearings-only target tracking*, IEEE Transactions on Signal Processing, **65**(23) (2017), 6119-6134.

[18] J. Passerieux, D. Pillon, P. Blanc-Benon, C. Jauffret, *Target motion analysis with bearings and frequencies measurements via instrumental variable estimator (passive sonar)*, Acoustics, Speech, and Signal Processing, International Conference on. IEEE, (1989), 2645-2648.

[19] H. W. Quan, *Target tracking using extended Kalman filter with bearing and Doppler measurements*, Applied Mechanics and Materials, **529** (2014), 379-382.

[20] B. Raeisy, A. A. Safavi, A. R. Khayatian, *Optimized fuzzy control design of an autonomous underwater vehicle*, Iranian Journal of Fuzzy Systems, **9**(2) (2012), 25-41.

[21] A. Rahimi, K. D. Kumar, H. Alighanbari, *Enhanced adaptive unscented Kalman filter for reaction wheels*, IEEE Transactions on Aerospace and Electronic Systems, **51**(2) (2015), 1568–1575.

[22] U. Rajyalakshmi, R. P. Mallikarjuna, D. Lingaraju, *Doppler-Bearing passive target tracking system for underwater target detection using modified gain EKF*, International Journal on Intelligent Electronic Systems, **5(2)**(2011), 12-17.

[23] A. Rosenqvist, *Asymptotic theory for a two-step pseudo-linear Doppler-bearing tracker*, Computational statistics and data analysis, **21**(6) (1996), 647-660.

[24] M. N. Santhosh, S. K. Rao, R. P. Das, K. L. Raju, *Underwater target tracking using unscented Kalman Filter*, Indian Journal of Science and Technology, **8**(31) (2015), 1-5.

[25] H. E. Soken, C. Hajiyev, *Adaptive unscented Kalman filter with multiple fading factors for pico satellite attitude estimation*, Recent Advances in Space Technologies, (2009), 541-546.

[26] H. E. Soken, C. Hajiyev, *Adaptive fading UKF with Q-adaptation: application to picosatellite attitude estimation*, Journal of Aerospace Engineering, **26**(3) (2011), 628-636.

[27] X. J. Tao, C. R. Zou, Z. Y. He, *Passive target tracking using maximum likelihood estimation*, IEEE Transactions on Aerospace and Electronic Systems, **32**(4) (1996), 1348-1354.

[28] V. Teuliere, O. Brun, *Parallelisation of the particle filtering technique and application to doppler-bearing tracking of maneuvering sources*, Parallel Computing, **29**(8) (2003), 1069-1090.

[29] R. Turner, C. E. Rasmussen, *Model based learning of sigma points in unscented Kalman filtering*, Neurocomputing, **80** (2012), 47-53.

[30] D. Wang, H. Lv, J. Wu, *In-flight initial alignment for small UAV MEMS-based navigation via adaptive unscented Kalman filtering approach*, Aerospace Science and Technology, **61** (2017), 73-84.

[31] C. Yang, J. Collins, *Improvement of honey bee tracking on 2D video with hough transform and Kalman filter*, Journal of Signal Processing Systems, **90**(12) (2018), 1639-1650.

[32] H. Yang, W. Li, C. m. Luo, *Fuzzy adaptive Kalman filter for indoor mobile target positioning with INS/WSN integrated method*, Journal of Central South University, **22**(4) (2015), 1324-1333.

[33] L. Yang, M. Sun, K. Ho, *Doppler-bearing tracking in the presence of observer location error*, IEEE Transactions on Signal Processing, **56**(8) (2008), 4082-4087.

[34] R. Zhan, J. Wan, *Iterated unscented Kalman filter for passive target tracking*, IEEE Transactions on Aerospace and Electronic Systems, **43**(3) (2007), 1155-1163.

[35] Q. Zhang, T. L. Song, *Improved bearings-only target tracking with iterated Gaussian mixture measurements*, IET Radar, Sonar and Navigation, **11**(2) (2016), 294-303.

[36] H. Zhou, H. Huang, H. Zhao, X. Zhao, X. Yin, *Adaptive unscented Kalman filter for target tracking in the presence of nonlinear systems involving model mismatches*, Remote Sensing, **9**(7) (2017), 657.

[37] H. Zhu, H. Hu, W. Gui, *Adaptive unscented kalman filter for deep-sea tracked vehicle localization*, Information and Automation, (2009), 1056-1061.